Published in IET Electric Power Applications
Received on 30th March 2012
Revised on 17th December 2012
Accepted on 2nd January 2013
doi: 10.1049/iet-epa.2012.0105

ISSN 1751-8660

Effect of open stator slots on the performance of an interior permanent magnet automotive alternator

Vlatka Životić-Kukolj[1,2], *Wen Liang Soong*[1]

[1]*University of Adelaide, School of Electrical and Electronic Engineering, Adelaide, SA 5005, Australia*
[2]*School of Computer Science, Engineering and Mathematics, Flinders University, Bedford Park, SA 5042, Australia*
E-mail: vlatka.zivotickukolj@flinders.edu.au

Abstract: This work describes a study of the effect of using open stator slots in an interior permanent magnet automotive alternator to increase its effective air gap and thus reduce its iron losses under field-weakening conditions. Analytical, finite-element and experimental results are compared for the back-electromotive waveforms, inductance saturation/torque curves, iron loss and field-weakening performance characteristics for the alternator with both semi-closed and with open slots. It is shown for the highly saturated machine considered, that using open stator slots can reduce the field-weakening iron loss without significantly affecting the machine performance.

1 Introduction

Permanent magnet (PM) generators offer the potential for high-power density, high-efficiency and a wide field-weakening (constant power) operating range. An interior PM concept demonstrator for a 6 kW automotive alternator was built and tested [1]. This demonstrated the desired wide speed range, but had poor efficiency because of high iron loss during field-weakening operation. Previous researchers have shown that these stator iron losses are because of high-amplitude, high-frequency air gap harmonics caused by the stator *d*-axis magnetomotive force (mmf) interacting with the salient rotor structure [2–5].

There has been strong recent interest in methods for reducing stator iron losses in PM machines under field-weakening operation. These have largely focused on modifying the rotor geometry to make the air gap flux density waveform more sinusoidal by adjusting the rotor barrier locations [6–8] or by changing the barrier shape and adding slots near the ends of the barriers [9]. Design rules for selecting the number of stator slots were also proposed in [7] to minimise the coupling of the air gap harmonics into the stator teeth.

Given that the stator tooth iron losses are because of stator *d*-axis mmf, these can be reduced by increasing the effective air gap length [4]. This will of course reduce also the PM and reluctance torque components producing a trade-off between the field-weakening iron loss and the low-speed torque capability.

In an earlier paper [10], the authors investigated three design changes to the 6 kW interior PM automotive alternator using finite-element analysis (FEA) and showed that increasing the effective air gap by changing the semi-closed stator slots to open slots had the most significant effect on the iron loss. This previous paper only showed the effect of changing to open slots on the iron loss against speed characteristic. In this present paper, a detailed comparison of the characteristics of the interior PM machine with semi-closed and open slots are presented including the back-electromotive force (back-EMF) waveform, inductance saturation curves, torque, flux density waveform, short-circuit loss and efficiency using analytical, finite-element and experimental methods.

In this paper, Section 2 describes the modelling and testing of the semi-closed and open-slot machine designs. In Section 3, a detailed back-EMF analysis was performed. Section 4 covers a study of the inductance and torque characteristics, whereas Section 5 discusses the short-circuit iron losses. Section 6 provides the load testing results followed by the conclusions in Section 7.

2 Modelling and testing

2.1 Machine design and finite-element modelling

An earlier paper [1] described the design and preliminary testing of the interior PM alternator. The machine uses a commercial 415 V, 4.8 A, 2.2 kW, 1410 rpm, four-pole induction motor stator which was not modified in any way. The (short-term) output power capability of this stator was increased from 2.2 to over 6 kW by using a custom-designed interior PM rotor, operating the machine at a current of 9.4 A, and increasing the operating speed to 4000 rpm. The higher operating current was chosen to produce an electric loading which is more representative of the high-performance, liquid-cooled machines typically used in automotive applications. Given that only air cooling was used during the testing process, the high operating current caused the stator winding temperature to rapidly increase and so restricted the allowable testing time to a few

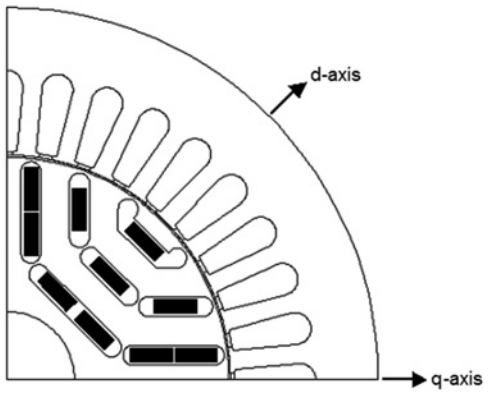

Fig. 1 *Cross-section of the rotor and stator laminations*

Table 1 Interior PM alternator machine design information

Parameter	Value	Parameter	Value
stack length	95 mm	air gap	0.39 mm
stator outer diameter	153 mm	magnet type	NdFeB
stator number of slots	36	rated voltage/ current	415 V/ 9.4 A
stator slot opening	2.49 mm	frequency	50 Hz
rotor outer diameter	92 mm	number of poles	4

minutes. Substantially improved cooling would clearly be required for the machine to operate continuously at this current level.

A quarter cross-section of the rotor and stator lamination showing the location of the sintered rare-earth rotor magnets is shown in Fig. 1. The rotor has three flux-barriers per pole. Each rotor pole has ten small bridges which mechanically retain the magnets at high speed.

The commercial induction machine stator used Polycor laminations, whereas the rotor was constructed from Lycore 150 laminations. The detailed design information of the machine design is presented in Table 1.

The Flux2D FEA modelling package was used to examine the air gap flux density distribution in the machine. Owing to symmetry reasons, only a quarter of the machine needed to be analysed and the model had around 23 000 elements. The machine had high iron loss in the stator teeth and it was found that cutting the tips of the stator teeth to form open slots reduced this. This means that the stator slot openings were widened. Note that the use of open slots will have implications for the mechanical retention of the windings in the slots.

2.2 Production of open stator slots

Fig. 2 illustrates the experimental procedure used to convert the semi-closed slots to open slots. Fig. 2*a* shows the original semi-closed slots. In Fig. 2*b*, the stator winding was first heated to soften the varnish and then compressed to move the winding away from the air gap by a couple of millimetres to allow the tips of the stator teeth to be removed by machining (Fig. 2*c*) without damaging the stator winding. Tests were performed on the machine at each of the three stages: semi-closed slots 'before compression' and 'after compression' and with the open slots.

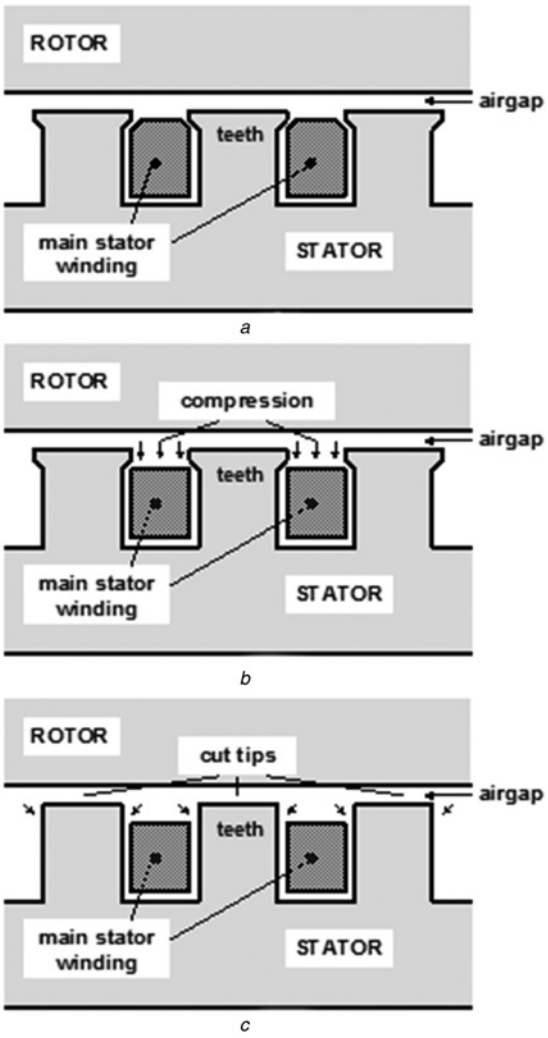

Fig. 2 *Diagrams showing*

a Original semi-closed stator slots
b After compression of stator winding
c After cutting of stator teeth tips producing open slots

Fig. 3 shows photographs of the original stator with semi-closed slots and the stator after cutting the tooth tips. The heating process used to soften the varnish has darkened the winding insulation, but should have no impact on the machine performance. In both cases, search coils were added to allow stator tooth flux measurements to be performed and compared with the FEA calculated results.

2.3 Experimental testing

In the experimental test arrangement, the interior PM alternator was driven by two parallel-connected 5 kW, 1.5 krpm DC motors through a belt drive with adjustable gear ratios of 1:1, 1:2 and 1:4, which produces a maximum mechanical power of 10 kW and maximum speed of 6 krpm. A 220 V/50 A variable DC power supply was used to drive the DC motors. The alternator torque was measured using a 25 Nm reaction torque transducer. The three-phase output voltages and currents, and the total electrical output power was measured.

Under open-circuit conditions, the input mechanical power consists of the open-circuit iron losses (plus friction and windage losses, which are assumed to be small).

doi: 10.1049/iet-epa.2012.0105

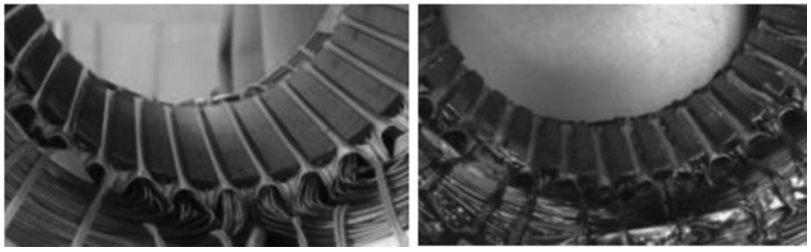

Fig. 3 *(Left) original stator with semi-closed slots, and (right) after compression and machining to produce open slots*

The experimental short-circuit iron loss was obtained by subtracting the copper losses (calculated from the measured stator current) from the input mechanical power required when driving the machine with the stator terminals short-circuited.

For the emulation of the electrical load on the alternator, a three-phase variable-resistance load was connected to the alternator terminals to model the input characteristics of a rectifier that is commonly used in automotive applications. Under the resistive load operation, the iron losses were obtained by subtracting the copper losses and the electrical output power from the input mechanical power. The stator resistance used in the calculations corresponded to the estimated winding operating temperature.

3 Back-EMF

The open-slot design has larger stator slot openings and hence a larger Carter's coefficient than the original semi-closed design. This results in an increase of the effective air gap of the machine and so reduces the open-circuit air gap flux density. This in turn reduces the back-EMF voltage and hence the PM contribution of the output torque.

Fig. 4 presents the finite-element calculated line back-EMF waveforms and their frequency spectra for the original semi-closed slot design against the open-slot design. Increasing the stator slot opening causes a small relative drop in the fundamental component of the back EMF and a substantial relative increase in the higher harmonics, in particular the 17th and 19th. This is expected as these correspond to the lowest-frequency tooth harmonics, and the higher tooth-slot permeance variation with the open slots is expected to increase the magnitude of these harmonic components.

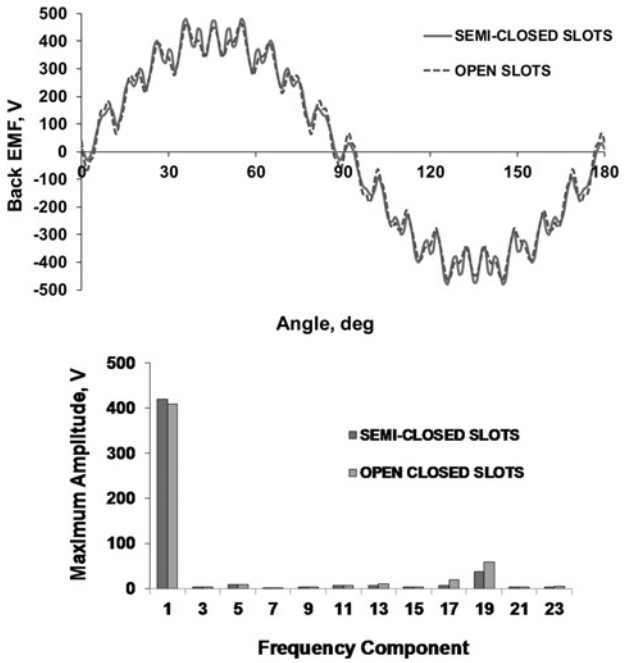

Fig. 4 *Calculated line back-EMF waveforms: (top) semi-closed design against open-slot design at 1500 rpm and (bottom) their frequency spectra*

Table 2 presents a comparison of the calculated and measured values of the line back-EMF voltages at 1500 rpm with semi-closed slots before and after compression of the stator winding, and with open slots. For the original machine, there is a 10% difference in the measured against calculated back-EMF voltages. This is likely to be because of the magnet remanent flux being lower and/or the air gap length being higher than expected. The compression of the stator winding has no impact on the value of the back EMF as expected. With changing to open slots, the measured reduction in the back-EMF (9 V) is comparable with the predicted reduction (7 V).

4 Inductances and torques

The larger effective air gap of the open-slot design will reduce both the *d*- and *q*-axis inductances of the machine design and hence affect the reluctance contribution of the output torque.

The machine has both high electric and magnetic loading and hence shows strong saturation and a significant cross-saturation effect between the *d*-axis magnet flux and the *q*-axis inductance. To examine the cross-saturation effect, two cases will be considered: firstly, performance of the rotor without any magnets (reluctance rotor) and then with the rare-earth rotor magnets (interior PM rotor). In the following, it is assumed that the *q*-axis is the high-inductance axis for both the reluctance and interior PM configurations.

4.1 Reluctance rotor inductances

The application of analytical methods can give useful insights into the effect of changing the stator slot opening on the machine inductances. Table 3 shows the analytical

Table 2 Calculated and measured line back EMFs

Back EMF, V_{rms}, J	Method	
	FEA	measured
with semi-closed slots	300	273
with semi-closed slots after compression	–	273
with open slots	293	264

Table 3 Reluctance rotor

Parameter	Semi-closed slots	Open slots
Carter's coefficient	1.315	1.507
actual air gap, mm	0.39	0.39
effective air gap g'', mm	0.513	0.588
magnetising inductance L_m, mH	373	325
slot-leakage inductance L_{slot}, mH	7.0	3.6
end-winding inductance L_{end}, mH (from test)	5.6	5.6
intrinsic d-axis magnetising ind. L_{dmi}, mH	21	21
q-axis inductance $L_q = L_m + L_{slot} + L_{end}$, mH	386	334
d-axis inductance $L_d = L_{dmi} + L_{slot} + L_{end}$, mH	33.6	30.2

Analytically calculated inductances

inductance calculations for a reluctance rotor using the approach described in [11]. The results presented include the end-winding inductance, which was previously empirically determined [12]. The calculated FEA inductances are presented in Fig. 5, whereas a comparison of the analytical, FEA and measured results is presented in Table 4 and uses the inductance measurement method described in [12]. The semi-closed slot stator was tested first using the rotor without magnets and then with magnets. The rotor magnets were then glued in place to improve mechanical integrity at high speeds. This, however, meant they could not then easily be removed for the reluctance rotor test with the open-slot stator and so experimental results for this case are not available.

Table 3 shows that changing to open slots firstly increases the Carter's coefficient from 1.315 to 1.507. This increases the value of the effective air gap of the machine by 15%, from 0.513 to 0.588 mm, and so reduces the magnetising inductance in the q-axis, from 373 to 325 mH. Secondly, the wider slot opening nearly halves the slot leakage inductance, from 7 to 3.6 mH.

These two effects cause a reduction in the analytically calculated unsaturated q-axis inductance from 386 to 334 mH. These results show a good match with the q-axis finite-element calculated results shown in Fig. 5. With increasing stator current the difference between the semi-closed and the open-slot designs becomes smaller because of heavy saturation in the stator teeth. Table 4

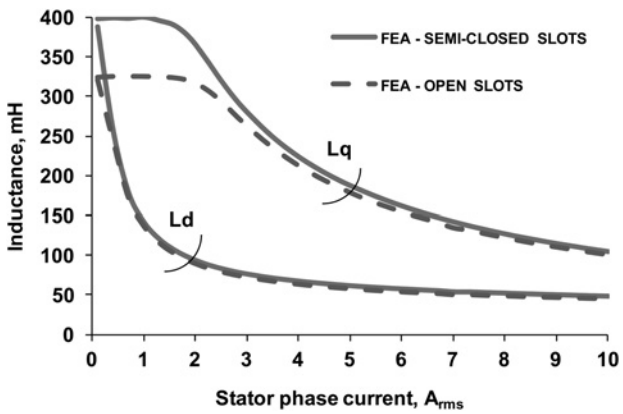

Fig. 5 *Reluctance rotor*

Calculated (FEA) inductance curves for semi-closed and open-slot machines

Table 4 Reluctance rotor

Inductance, mH	Semi-closed slots			Open slots		
	Analyt.	FEA	Exp.	Analyt.	FEA	Exp.
L_q (unsat)	380	399	355	329	324	–
L_q (sat)	–	104	100	–	101	–
L_d (unsat)	380	389	331	329	320	–
L_d (sat)	34	48	58	30	46	–

Comparison of the L_d and L_q parameters under unsaturated (0.5 A) and saturated (9.4 A) conditions for the analytical, finite-element and test results

shows that the experimental measurements with the semi-closed stator slots show a significantly lower value of unsaturated q-axis inductance but a comparable value for the saturated value. This is consistent with the actual air gap being slightly larger than expected.

The observed phenomenon in the d-axis is of a different nature. At low stator currents the rotor bridges are unsaturated and the reluctance rotor is equivalent to a solid rotor where the values of q- and d-axis inductances are similar. As the rotor bridges are narrow, they saturate very quickly as the stator current increases, causing a dramatic drop in the d-axis inductance as shown in Fig. 5. Table 3 shows for the open-slot design, the increase of the Carter's coefficient has little impact on the d-axis magnetising inductance because of the large air gap associated with the rotor magnets; however, the decrease in slot leakage does cause a 10% reduction in the calculated analytical d-axis inductance. Table 4 shows that the FEA predicts a 5% reduction.

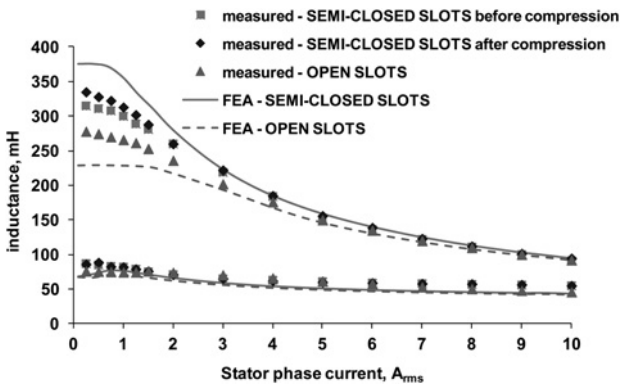

Fig. 6 *Interior PM rotor*

Calculated FEA (lines) and measured (symbols) inductance curves for semi-closed and open-slot machines

Table 5 Interior PM rotor

Inductance, mH	Semi-closed slots			Open slots		
	Analyt.	FEA	Exp.	Analyt.	FEA	Exp.
L_q (unsat)	380	377	312	329	228	278
L_q (sat)	–	97	92	–	98	92
L_d (unsat)	34	61	83	30	55	76
L_d (sat)	34	44	53	30	41	46

Comparison of the L_d and L_q parameters under unsaturated (0.5 A) and saturated (9.4 A) conditions. The semi-closed experimental results are those before compression

doi: 10.1049/iet-epa.2012.0105

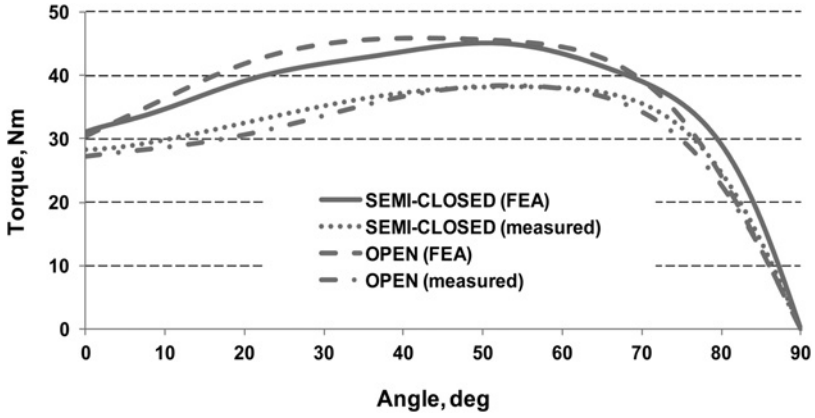

Fig. 7 *Calculated torque against current angle based on back-EMF and inductance saturation curves using calculated parameters (FEA) and measured parameters for semi-closed and open-slot stators with interior PM rotor*

4.2 Interior PM rotor inductances

Inserting the PMs into the reluctance rotor produces the interior PM rotor. The strong magnet flux from the rare-earth magnets in the *d*-axis saturates the rotor bridges reducing the unsaturated *d*-axis inductance. It also causes cross-saturation in the *q*-axis reducing the unsaturated *q*-axis inductance. Comparisons of the finite-element and experimental inductance saturation curves are given in Fig. 6 and Table 5. The finite-element *d*-axis inductance was obtained based on the difference between the *d*-axis flux-linkage with a given value of stator current and the open-circuit *d*-axis flux-linkage.

Fig. 6 shows the FEA inductance predictions for the semi-closed slots before and after compression, and for the open slots with the interior PM rotor. Compression of the stator winding pushes the stator coils towards the bottom of the stator slot and so increases the slot-leakage inductance and hence both the *d*- and *q*-axis inductances. However, the increase in the inductances after compression, particularly for the *q*-axis, is much larger than the *d*-axis. This is unexpected as only the slot leakage inductance should be changed by the compression and hence the increase was expected to be the same in each axis. The measured effect could be explained by the force used to compress the winding also causing the stator teeth to become slightly narrower and longer, and so producing a small reduction in the air gap.

Cutting the stator tooth tips to produce open slots reduces both the magnetising and leakage inductances causing the *d*- and *q*-axis inductances to drop as discussed above. The drop in the *q*-axis inductance is larger than the *d*-axis inductance because of the larger magnetising inductance in this axis.

The rotor magnets in the *d*-axis saturate the rotor bridges. This causes a large drop in the calculated FEA unsaturated *d*-axis inductances for the semi-closed slot stator from 389 to 61 mH and for the open-slot stator from 320 to 55 mH. The rotor magnets cause a 10% reduction in the saturated *d*-axis inductance.

The rotor magnet *d*-axis flux causes saturation of the stator teeth. This reduces the *q*-axis flux and hence produces a significant drop of the *q*-axis inductance (cross-saturation). For the semi-closed slot stator design, cross-saturation causes a drop of the calculated FEA unsaturated *q*-axis inductance from 399 to 377 mH. In the open-slot stator, cross-saturation is even more significant and the calculated FEA unsaturated inductance drops from 324 to 228 mH. However, at high *q*-axis currents the effect of cross-saturation on L_q is small.

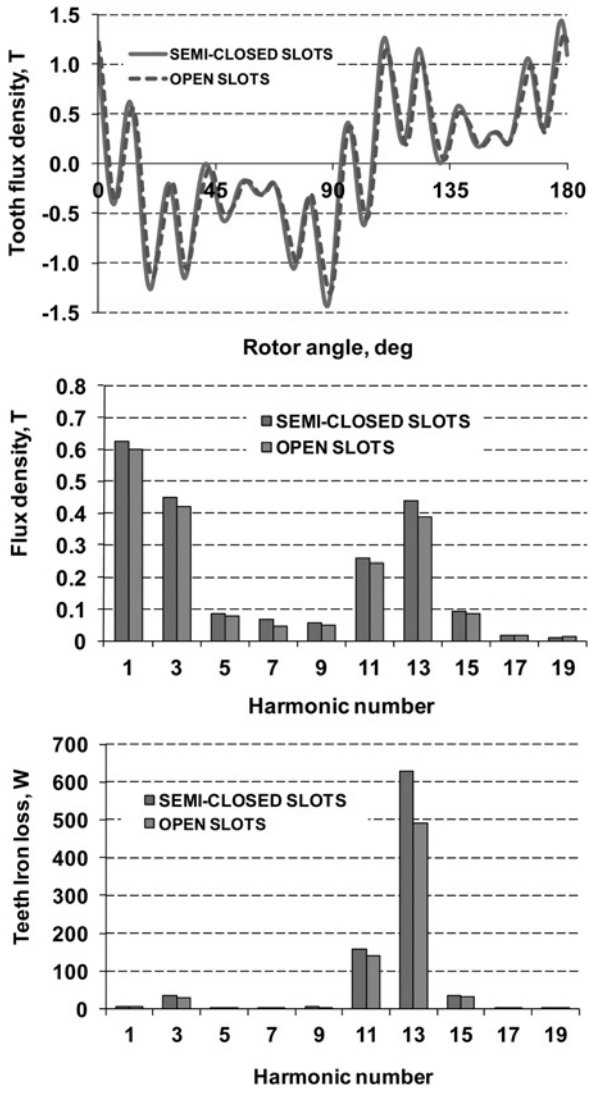

Fig. 8 *Calculated FEA stator tooth short-circuit iron losses for semi-closed and open-slot designs*

Tooth flux density against rotor angle (top), its harmonic components (middle) and teeth eddy-current harmonic loss components at 6000 rpm (bottom)

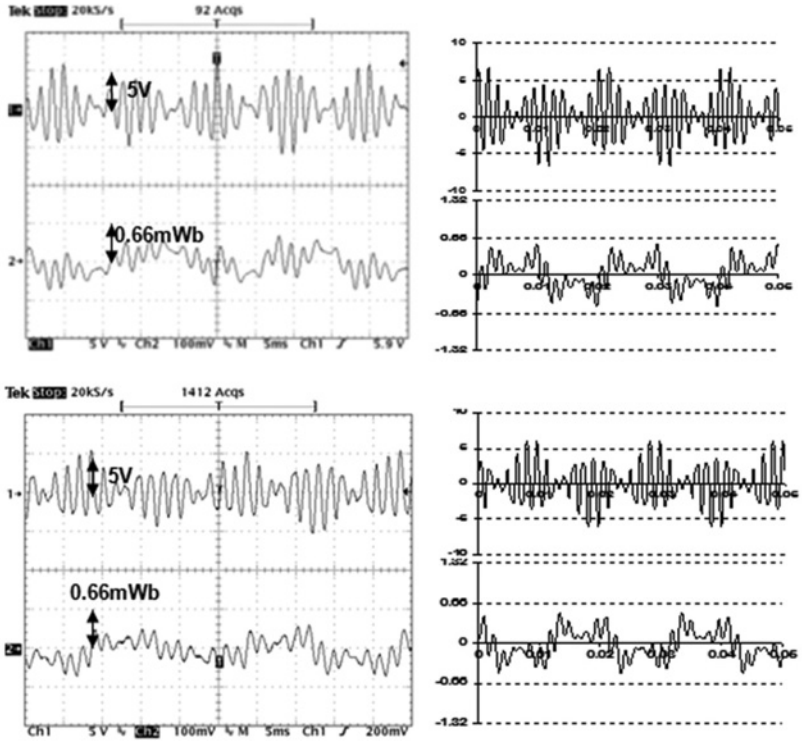

Fig. 9 *Search coil-induced voltage (upper subplots) and corresponding stator tooth flux waveform (lower subplots) at 1500 rpm*
Semi-closed (upper row) against open-slot design (lower row) – (Left) measured and (right) calculated from FEA

4.3 Interior PM rotor torque comparison

Fig. 7 presents the calculated torque against current angle curves for the semi-closed and open-slot stators with the interior PM rotor. They were calculated firstly from the FEA back-EMF and inductance saturation curves and secondly from the measured back-EMF and inductance saturation curves.

The measured parameters show both a significantly lower calculated magnet torque because of the lower measured back-EMF, and a reduced calculated reluctance torque because of a smaller difference between the *q*- and *d*-axis inductances (see Fig. 6). The maximum torque predicted by the measured parameters for the semi-closed stator, about 38 Nm, is comparable to the measured value of about 40 Nm obtained in earlier tests [1].

The results show no significance difference in the maximum torque capability of the machine between semi-closed and open slots despite the larger effective air gap. The open-slot design has a slightly lower magnet air gap flux and hence magnet torque, as shown by the torque at zero-current angle, but this is compensated for by the reduction in saturation increasing the reluctance torque.

5 Short-circuit iron losses

The effect of using open slots against semi-closed slots on the short-circuit iron loss was investigated using FEA. The stator tooth iron loss was obtained using the instantaneous tooth flux density against time waveforms and the stator lamination iron loss characteristics [10]. The tooth flux density was obtained by averaging over the width of the tooth and assumed constant over the entire tooth. This is a reasonable approximation for the parallel-sided teeth, but could not be applied accurately to the stator yoke.

From examining the stator flux density plots under short-circuit conditions, it was found that the highest flux densities occurred in the stator teeth, whereas the stator yoke flux density was very low (see [10]). This observation is that the most of the stator loss under short-circuit conditions occurs in the stator teeth is consistent with earlier work [2–5].

It was found that using open slots in the machine design significantly reduces the iron losses in the stator teeth under field-weakening operation. Fig. 8 presents a comparison of the semi-closed and open-slot stator designs in regards to tooth flux density and harmonic components of the calculated tooth flux density and eddy-current loss at 6000 rpm.

The stator tooth flux density waveforms under short-circuit conditions show large-amplitude harmonics. The eddy-current losses are proportional to the square of both the frequency (harmonic number) and the amplitude of the flux density harmonics. Thus Fig. 8 shows it is the high-frequency, high-amplitude flux density harmonics that produce the largest stator tooth iron loss. The 13th harmonic component is dominant and represents the majority of the total eddy-current losses; the second largest component is the 11th harmonic.

The open-slot design shows lower harmonic amplitudes compared to the semi-closed design, for the instance the 11th harmonic flux density component reduces by 6%, whereas the 13th harmonic component reduces by 11%. This produces a significant reduction in the high-order harmonic losses, for instance the 13th harmonic loss drops from 630 to 490 W, a 23% reduction.

Given that the harmonic losses are associated with stator armature reaction fields, increasing the slot opening [4] and hence increasing the effective air gap would be expected to reduce the magnitude of these fields. From Table 3 shown

doi: 10.1049/iet-epa.2012.0105

earlier, it was found that the effective air gap increased by about 15% because of the increased value of Carter's co-efficient. This value shows a reasonable correspondence with the reduction (11%) in the 13th harmonic component which is the main loss component.

5.1 Measured short-circuit losses

Fig. 9 presents a comparison of the calculated and measured search coil voltage and tooth flux for the semi-closed and open-slot interior PM machines under the short-circuit condition at 1500 rpm (50 Hz). These show that under short-circuit conditions the fundamental component of the tooth flux is small and large harmonic components appear. The latter are associated with high iron losses. The FEA results show a good correspondence in the magnitudes and shapes of the calculated against measured waveforms for both designs.

Fig. 10 presents a comparison of the calculated stator tooth iron losses and the measured total stator iron losses under short-circuit conditions as a function of speed. The method used to segregate the stator iron losses from the measured mechanical input power was described in Section 2.3. It shows that the measured total short-circuit iron losses are close to the calculated iron losses for the stator teeth alone for both designs. This is because the majority of the high stator flux density regions under the short-circuit condition are concentrated in the stator teeth (see [10]). In changing to open slots, the measured short-circuit iron loss reduction is about 21% (averaged over speeds from 3000 to 6000 rpm), which compares well with the finite-element prediction of 19%.

Fig. 11 presents the measured short-circuit current against speed with semi-closed and open slots. It can be seen that compression of the stator winding did not cause significant changes in the short-circuit current, however, an increase in the short-circuit current occurred after the slots were opened. This was expected as with open slots, the *d*-axis inductance decreased more than the back-EMF magnitude.

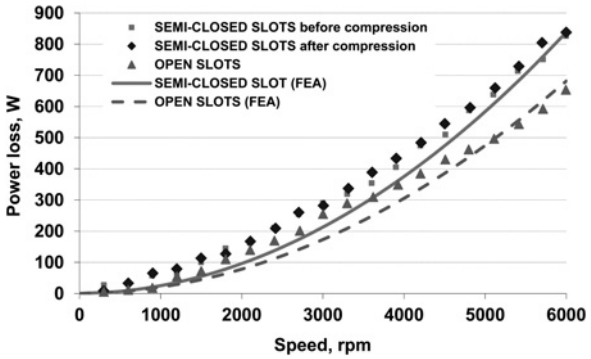

Fig. 10 *Comparison of short-circuit iron losses against speed showing the stator tooth iron loss finite-element predictions and total stator iron loss measurements for the semi-closed and open-slot designs*

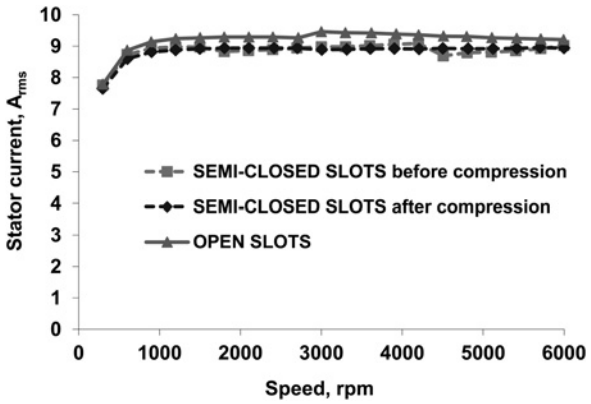

Fig. 11 *Measured short-circuit current against speed with semi-closed slots (before and after compression) and with open slots*

6 Performance testing

The measured stator current, electrical power output and efficiency against speed for the semi-closed and open-slot designs are presented in Fig. 12 for the alternator operating into a three-phase resistive load. The resistive load consisted of three adjustable (switched) resistive load banks rated at 240 V/20 A. At each speed, its resistance value was adjusted to maximise the electrical output power.

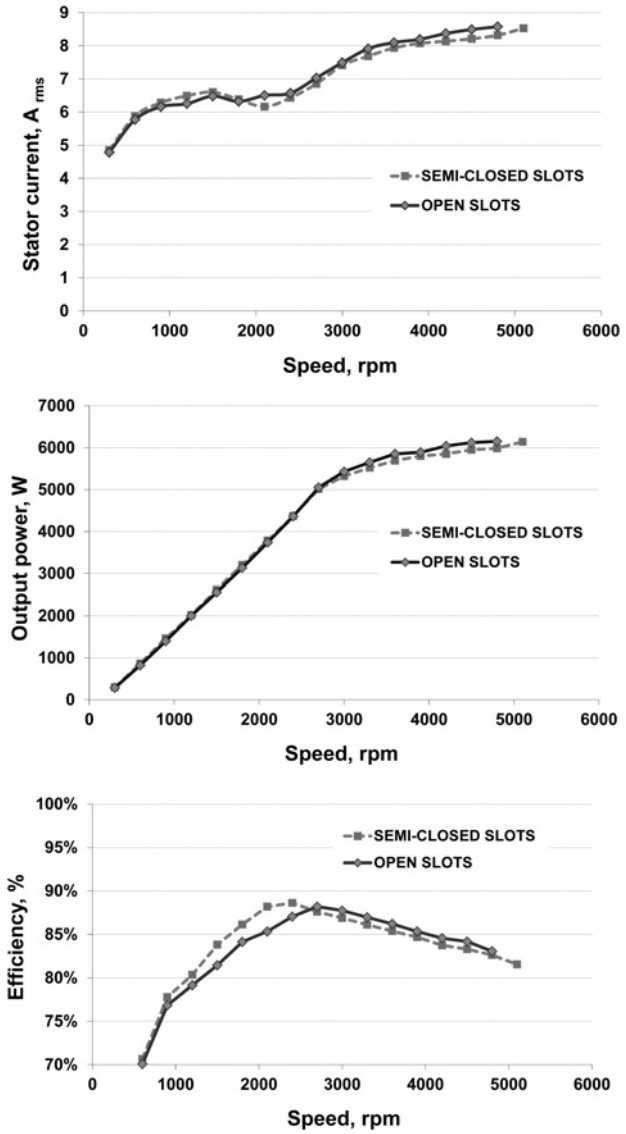

Fig. 12 *Measured stator current, electrical power output and efficiency against speed for semi-closed and open slots*

Rated speed, when the output voltage reaches its rated value, occurs at about 2700 rpm. Below the rated speed, the maximum power is ideally achieved with a stator current equal to the short-circuit current divided by $\sqrt{2}$ [13], which is about 6.6 A. At very low speeds, the effects of stator resistance cause the stator current to fall. Above rated speed, the stator current increases and asymptotes towards the short-circuit current.

For the open-slot design, it was experimentally confirmed that the short-circuit current increases slightly, so an increase in stator current above rated speed was expected and is observed in Fig. 12. This has two effects, firstly it increases the output power (about 3%), but secondly it also increases the stator copper loss. The net effect is that the efficiency shows only a relatively small improvement (about 1%) compared with the semi-closed slot design.

Below rated speed, the majority of the losses in the machine are caused by stator copper loss. The increase in the short-circuit current would be expected to increase the stator current, stator copper loss and hence reduce the efficiency below rated speed. Although the measured efficiency does show a reduction in this range, the stator current does not show a significant increase which is surprising. Further investigation of this result is required.

7 Conclusions

This paper examined increasing the effective air gap of an interior PM automotive alternator to reduce the stator iron losses under field-weakening operation. The effective air gap was increased by changing from semi-closed to open-stator slots. Analytical and finite-element analyses and experimental tests were used. The main findings were as follows:

- Using open-stator slots reduced the measured back-EMF voltage by 4% because of the increased Carter's coefficient, and also reduced the saturated *d*-axis inductance by 13% because of the lower stator slot leakage and hence increased the short-circuit current.
- From the calculated torque against angle characteristics based on the calculated and measured parameters, the change of stator slot opening had no significant impact on the total torque. This is likely because of the decrease in back-EMF and hence magnet torque being offset by a reduction in saturation and hence increase in reluctance torque.
- The increased effective air gap reduced the stator tooth harmonic flux densities and caused the measured short-circuit iron loss to reduce by 21% at high speeds, this showed a good correspondence with the finite-element prediction of 19%.
- The output power against speed and efficiency against speed characteristics both improved slightly at high speeds.

Thus, for the heavily saturated interior PM machine considered, the field-weakening iron loss can be reduced significantly by increasing the effective air gap without affecting the low-speed output torque. Although the primary method for reducing this field-weakening iron loss is still through optimisation of the rotor geometry [6–9], increasing the effective air gap length is another variable, which can be considered in the design process.

8 Acknowledgments

This work was supported by the Australian Research Council Discovery grants, DP0342874 and DP0988255. Technical support from the staff of the School of Electrical and Electronic Engineering's mechanical workshop during the experimental testing is gratefully acknowledged. We also thank T.J.E. Miller for providing the Polycor lamination data and the reviewers for their valuable feedback.

9 References

1 Soong, W.L., Ertugrul, N.: 'Inverterless high-power interior permanent-magnet automotive alternator', *IEEE Trans. Ind. Appl.*, 2004, **4**, (40), pp. 1083–1091
2 Schiferl, R., Lipo, T.A.: 'Core loss in buried magnet permanent magnet synchronous motors', *IEEE Trans. Energy Convers.*, 1989, **4**, (2), pp. 279–284
3 Zhu, Z.Q., Chen, Y.S., Howe, D.: 'Iron loss in permanent-magnet brushless AC machines under maximum torque per ampere and flux weakening control', *IEEE Trans. Magn.*, 2002, **38**, (5), pp. 3285–3287
4 Magnussen, F., Chin, Y.K., Soulard, J., Broddefalk, A., Eriksson, S., Sadarangani, C.: 'Iron losses in salient permanent magnet machines at field-weakening operation'. IEEE Industry Applications Conf., ICEM 2004, no. 1, pp. 40–47
5 Yamazaki, K., Seto, Y.: 'Iron loss analysis of interior permanent-magnet synchronous motors-variation of main loss factors due to driving condition', *IEEE Trans. Ind. Appl.*, 2006, **42**, (4), pp. 1045–1052
6 Kamiya, M.: 'Development of traction drive motors for the Toyota hybrid system', *IEEJ Trans. Ind. Appl.*, 2006, **126**, (4), pp. 473–479
7 Han, S.-H., Soong, W.L., Jahns, T.M., Guven, M.K., Illindala, M.S.: 'Reducing harmonic eddy-current losses in the stator teeth of interior permanent magnet synchronous machines during flux weakening', *IEEE Trans. Energy Convers.*, 2010, **25**, (2), pp. 441–449
8 Barcaro, M., Bianchi, N., Magnussen, F.: 'Rotor flux-barrier geometry design to reduce stator iron losses in synchronous IPM motors under FW operations', *IEEE Trans. Ind. Appl.*, 2010, **5**, (46), pp. 1950–1958
9 Yamazaki, K., Ishigami, H.: 'Reduction of harmonic iron losses in interior permanent magnet motors by optimization of rotor structures'. Int. Conf. Electrical Machines and Systems, ICEMS, 2008, pp. 2870–2875
10 Zivotic-Kukolj, V., Soong, W.L., Ertugrul, N.: 'Iron loss reduction in an interior PM automotive alternator', *IEEE Trans. Ind. Appl.*, 2006, **6**, (42), pp. 1478–1486
11 Soong, W.L.: 'Design and modeling of axially-laminated interior PM machines'. *PhD thesis*, University of Glasgow, UK, 1993
12 Zivotic-Kukolj, V.: 'Analysis of idle power and iron loss reduction in an interior PM automotive alternator'. PhD thesis, University of Adelaide, Australia, 2010
13 Pathmanathan, M., Soong, W.L., Ertugrul, N.: 'Output power capability of surface PM generators with switched-mode rectifiers'. IEEE Conf. on Sustainable Energy Technologies, ISCET, 2010, pp. 1–6

doi: 10.1049/iet-epa.2012.0105